

Realization of Odd-Frequency p -Wave Spin-Singlet Superconductivity Coexisting with Antiferromagnetic Order near Quantum Critical Point

Yuki FUSEYA, Hiroshi KOHNO and Kazumasa MIYAKE

Division of Materials Physics, Department of Physical Science, Graduate School of Engineering Science, Osaka University, Toyonaka, Osaka 560-8531, Japan

(Received March 27, 2021)

It is shown that the p -wave singlet superconductivity, whose gap function is odd both in momentum and in Matsubara frequency, is realized prevailing over the d -wave singlet state very close to the antiferromagnetic quantum critical point (QCP) both in the paramagnetic and in antiferromagnetic sides. Off the QCP in the paramagnetic phase, however, the d -wave singlet superconductivity with line-nodes is realized as *conventional* anisotropic superconductivity. This p -wave singlet superconductivity is an essentially gapless state, i.e., there is no gap in the quasiparticle spectrum everywhere on the Fermi surface due to its odd-frequency gap. These features can give a qualitative but nice understanding of the anomalous behaviors of NQR relaxation rate on CeCu_2Si_2 or CeRhIn_5 where the antiferromagnetism and superconductivity coexist on a microscopic level.

KEYWORDS: p -wave singlet superconductivity, gapless superconductivity, coexistence of antiferromagnetism and superconductivity, CeCu_2Si_2 , CeRhIn_5

1. Introduction

The discovery of the superconductivity in CeCu_2Si_2 ¹⁾ two decades ago triggered off a breakthrough in the field of superconductivity. Nowadays, we seem to have reached the consensus that the anisotropic spin singlet pairing, e.g. “ d -wave singlet” pairing, is realized in the superconducting (SC) states close to the antiferromagnetic (AF) states due to the AF spin fluctuations.²⁻⁵⁾ Recent developments on CeCu_2Si_2 , however, suggest that it still disguises much various physics.^{6-10, 13, 14, 18)} Polycrystalline sample of $\text{Ce}_{0.99}\text{Cu}_{2.02}\text{Si}_2$ shows a peak in the nuclear spin lattice relaxation rate $1/T_1$ at SC transition temperature $T_c \sim 0.65\text{K}$ and $1/T_1 \propto T$ behavior at $T \leq T_c$, which indicates essentially gapless superconductivity to be realized at $T < T_c$ at ambient pressure. At pressures $P \gtrsim 0.1\text{GPa}$, however, the $1/T_1 \propto T^3$ behavior, indicating line-node gap, is observed.⁶⁻⁸⁾ Since the Ge substitution for Si is considered to expand the lattice constant, giving negative pressure, 1% Ge substituted compound $\text{CeCu}_2(\text{Si}_{0.99}\text{Ge}_{0.01})_2$ exhibits AF ordering at $T < T_N = 0.75\text{K}$, followed by the onset of superconductivity at $T = T_c = 0.5\text{K}$ at ambient pressure. The observation of single component of NQR signal, showing an appearance of the internal field throughout the sample, excludes the possibility of phase segregation between the SC and the AF phases; namely, SC and AF coexist on a microscopic level. In this SC states, $1/T_1$ does not show any significant reduction below T_c , but shows essentially the same behavior as the normal Fermi liquid state. At

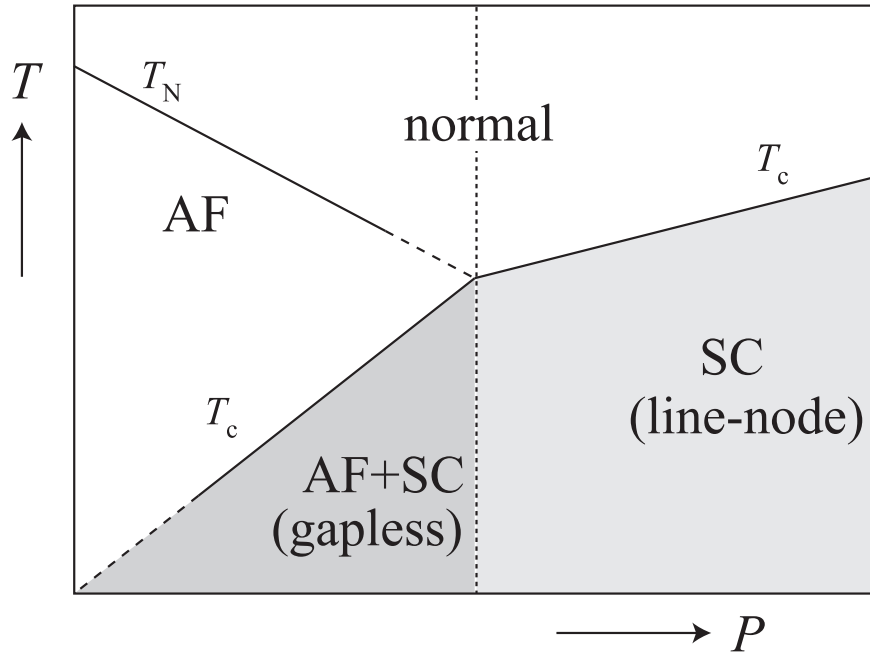


Fig. 1. Schematic phase diagram near the phase boundary between antiferromagnetic and superconducting states based on the NQR experiments on CeCu_2Si_2 and CeRhIn_5 .

$P = 0.85\text{GPa}$, on the other hand, it does not exhibit the AF ordering and the line-node SC gap evidenced from a clear behavior of $1/T_1 \propto T^3$.⁹⁾

Interestingly, the recently discovered pressure induced superconductor, CeRhIn_5 ¹⁵⁾ of Ce-based heavy fermion, shows features quite similar to those of CeCu_2Si_2 , while its crystal structure is rather two-dimensional compared to CeCu_2Si_2 . At ambient pressure, CeRhIn_5 shows AF ordering at $T < T_N = 3.8\text{K}$ and T_N exhibits a moderate variation for $P \lesssim 1.75\text{GPa}$, while the internal field H_{int} is linearly reduced in the region $0 < P < 1.23\text{GPa}$, suggesting that H_{int} vanishes at $P \simeq 1.6\text{GPa}$. At $P \sim 1.6\text{GPa}$, the SC state begins to appear, even though the AF ordering still exists.¹⁵⁻¹⁸⁾ The detailed NQR measurement shows that at $P = 1.75\text{GPa}$, the AF order and the SC order coexist on a microscopic level and $1/T_1$ in SC state exhibits essentially the same T -dependence as the normal state as is seen in CeCu_2Si_2 .¹⁶⁻¹⁸⁾ Under the pressures $P > 2.1\text{GPa}$, where the AF state disappears, the $1/T_1 \propto T^3$ behavior is observed as a usual singlet superconductivity with line-nodes.¹⁶⁾ The specific heat of CeRhIn_5 ¹⁹⁾ exhibits a feature consistent with the NQR measurement. At $P \sim 1.6\text{GPa}$, the specific heat shows a broad peak which is expected to be associated with the AF ordering at $T \sim 3\text{K}$, and shows a shoulder at $T \sim 2\text{K}$, which indicates the appearance of the gapless superconductivity. This shoulder grows to a mean-field like peak at $P \geq 1.9\text{GPa}$, which would be associated with the anisotropic singlet pairing.

Putting all these together, we can draw a schematic phase diagram near the phase boundary between AF and SC states as shown in Fig.1. The P - T phase diagram can be separated into

three parts: AF phase, SC phase and a coexisting phase of AF and SC ordering (AF+SC phase). This coexistence is quite different from that of UPd₂Al₃, in which plural f electrons, in $(5f)^3$ -configuration of U³⁺ ion, shows a dual character of correlated electrons. Of three f -electrons per U³⁺ ion, two electrons form essentially localized $5f^2$ -electron state, as in the U⁴⁺ state with singlet crystalline electric field ground state, while the remaining one electron forms the heavy Fermi liquid due to a larger hybridization with conduction electrons.²⁰⁾ In Ce-based heavy fermion compounds, on the other hand, there is only one $4f$ -electron per Ce³⁺ ion, and thus the same f -electron exhibits simultaneously itinerant and localized dual nature.²¹⁾ The qualitative difference of the manner of the coexistence of AF and SC can easily be seen by the property of $1/T_1$ on UPd₂Al₃²²⁾ and CeCu₂Si₂.^{6, 7, 9)}

A crucial aspect of the AF+SC phase is that the gapless superconductivity is realized, although the singlet pairing with line-node due to the antiferromagnetic fluctuation is expected to emerge. Although one can soon suspect that the origin of this gapless superconductivity is due to the impurity scattering, all the samples above are expected to be very clean. In fact, the clear $1/T_1 \propto T^3$ behavior is observed on the same sample under the pressures away from the boundary between AF+SC and SC phases. Even if the sample is very clean, there is still a possibility of the enhanced impurity scattering associated with quantum critical phenomena.²³⁻²⁵⁾ In such a case, however, T_c should be reduced considerably, while Ce_{0.99}Cu_{2.02}Si₂ at ambient pressure, exhibiting $1/T_1 \propto T$, does not show a clear decrease of T_c .⁶⁻⁸⁾ Therefore, the AF+SC phase in these Ce-based compounds seem to show the possibility of novel mechanism of “unconventional” superconductivity.

In this paper, we present a possible scenario to unravel these mysterious features observed in CeCu₂Si₂ and CeRhIn₅ near the boundary between AF+SC and SC phases. An essential idea here is that a gapless p -wave singlet superconductivity with the so-called odd-frequency gap, which is odd both in momentum and in frequency, should be realized very near the quantum critical point (QCP) and/or in the AF+SC phase. It depends on the specific property of the systems whether the boundary between AF+SC phase and SC phase corresponds to QCP or not. However, the present theory can apply to both cases. The Pauli principle requires that the spin singlet gap function must be even under simultaneous parity- and time-inversion operations. Therefore, there are two types of singlet gap function; the first one is even both in frequency and in momentum, the other is odd both in frequency and in momentum. The latter type of gap was proposed by Balatsky and Abrahams (BA) in the context of the research of high- T_c cuprates about a decade ago,²⁶⁾ after the proposal by Berezinskii for the model of superfluid ³He.²⁷⁾ BA argued that there is no gap in the quasiparticle spectrum with odd-frequency gap and these superconductors would still exhibit the Meissner effect, just as in the case of odd-energy gap proposed at very early stage of research as a model of CeCu₂Si₂ which was claimed to exhibit gapless nature of $1/T_1$.^{28, 29)} The model phonon interaction discussed by BA was shown to be an impractical one, and it was speculated without

specifying any explicit models that electron-electron interaction might mediate such odd frequency pairing in general.³⁰⁾

Here we show that a realistic model interaction mediated by the critical spin fluctuation can give rise to the odd-frequency gap superconductivity if the Fermi surface of quasi particles satisfies some mild condition. In the next section, we describe the model and formalism of solving a linearized gap equation to obtain the SC transition temperature T_c . In §3, we present the numerical results and discuss the condition that T_c of p -wave singlet superconductivity prevails over that of d -wave singlet superconductivity. In §4, we show that the obtained p -wave singlet SC state is really a gapless state also in real frequency space, i.e., $\Delta(\omega = 0) = 0$. In §5, we apply the same method to the region where the AF and SC order coexist and show the p -wave singlet superconductivity is also realized there. Then, we discuss the correspondence between results of our theory and experimental results. Section 6 is devoted to summary.

2. Model and Formulation

First we introduce the effective interaction taking into account the characteristic features of Ce-based compounds CeCu_2Si_2 and CeRhIn_5 near the boundary between the AF and SC phase. For this purpose, it may be useful to recall the fact that the SC transition temperature of CeCu_2Si_2 (CeRhIn_5) exhibits maximum at away from the phase boundary $P^* \sim 2.5\text{GPa}^{11,12)}$ (2.5GPa).

It was shown theoretically, on the standard approximation for an extended Anderson lattice model, that the maximum of T_c is raised by the critical valence fluctuations.¹³⁾ The recent experiment on $\text{CeCu}_2(\text{Si}_{0.9}\text{Ge}_{0.1})_2$ has revealed that the SC phase is separated into the phase near the phase boundary of AF phase and that around $P \sim P^*$.¹⁴⁾ So, it is natural to consider that the latter is due to the critical valence fluctuations and the former is due to the critical spin fluctuations. This would be also valid for the CeRhIn_5 which exhibits the analogous features with the CeCu_2Si_2 .³¹⁾ Upon this consideration, in order to discuss the mechanism of superconductivity near the phase boundary, we introduce the effective interaction $V(\mathbf{q}, i\omega_m)$ as the following phenomenological form mediated by spin fluctuations:

$$V(\mathbf{q}, i\omega_m) = g^2 \chi(\mathbf{q}, \omega_m) \equiv \frac{g^2 N_F}{\eta + A \hat{\mathbf{q}}^2 + C |\omega_m|}, \quad (1)$$

where g is the coupling constant, N_F the density of states at the Fermi level, and $\hat{\mathbf{q}}^2 \equiv 4 + 2(\cos q_x + \cos q_y)$ in two dimensions. This type of pairing interaction was adopted by Monthoux and Lonzarich to discuss the strong coupling effect on the superconductivity induced by the critical AF fluctuations.⁵⁾ One of the motivations of adopting $\hat{\mathbf{q}}^2$ as above is that the ordering vector \mathbf{Q} of AF phase in CeRhIn_5 was identified as $\mathbf{Q} = (1/2, 1/2, 0.297)$ by the neutron diffraction measurements,³²⁾ while that in $\text{CeCu}_2(\text{Si}_{0.99}\text{Ge}_{0.01})_2$ has not been identified yet. Another one is that calculations become much simpler in two dimensions than three dimensions while qualitative

physical picture is remained unchanged.

The linearized gap equation is given in a weak-coupling approximation as follows:

$$\Delta(\mathbf{k}, i\varepsilon_n) = -T \sum_{\mathbf{k}', \varepsilon'_n} \frac{V(\mathbf{k} - \mathbf{k}', i\varepsilon_n - i\varepsilon'_n)}{\xi_{\mathbf{k}'}^2 + |\varepsilon'_n|^2} \Delta(\mathbf{k}', i\varepsilon'_n), \quad (2)$$

where $\xi_{\mathbf{k}}$ is the dispersion of the quasiparticle, and the pairing interaction is given by (1). The pairing interaction can be decomposed as

$$V(\mathbf{k} - \mathbf{k}', i\omega_m) = \sum_l V_l(i\omega_m) \phi_l^*(\mathbf{k}) \phi_l(\mathbf{k}'), \quad (3)$$

where $\phi_l(\mathbf{k})$ is an irreducible representation of crystal group. The coefficient $V_l(i\omega_m)$ in (3) is given as

$$V_l(i\omega_m) = \sum_{\mathbf{k}, \mathbf{k}'} \phi_l(\mathbf{k}) V(\mathbf{k} - \mathbf{k}', i\omega_m) \phi_l^*(\mathbf{k}'). \quad (4)$$

In order to make our argument as simple and transparent as possible, we concentrate on the frequency dependence of the gap function and assuming the two-dimensional circular Fermi surface shown in Fig. 2. Then, the p - and d -wave components are retained:

$$V_l(i\omega_m) = \int \frac{d\mathbf{k}}{v_F} \frac{d\mathbf{k}'}{v_F} \phi_l(\mathbf{k}) V(\mathbf{k} - \mathbf{k}', i\omega_m) \phi_l^*(\mathbf{k}'), \quad (5)$$

$$\phi_p(\mathbf{k}) \equiv \Phi_p^{-1} N_F^{-1} \delta(\xi_{\mathbf{k}} - \mu) \sin k_{Fx} \quad (\equiv z_p^{-1} N_F^{-1} \delta(\xi_{\mathbf{k}} - \mu) \sin k_{Fy}), \quad (6)$$

$$\phi_d(\mathbf{k}) \equiv \Phi_d^{-1} N_F^{-1} \delta(\xi_{\mathbf{k}} - \mu) (\cos k_{Fx} - \cos k_{Fy}), \quad (7)$$

where the wave vector on the Fermi surface are expressed as $\mathbf{k}_F = (k_{Fx}, k_{Fy})$, and Φ_l is the normalization factor.

The linearized gap equation for each partial-wave component can be written in the form:

$$\lambda(T) \Delta_l(i\varepsilon_n) = -T \sum_{\mathbf{k}', \varepsilon'_n} \frac{V_l(i\varepsilon_n - i\varepsilon'_n)}{\xi_{\mathbf{k}'}^2 + |\varepsilon'_n|^2} \Delta_l(i\varepsilon'_n). \quad (8)$$

Assuming $\xi_{\mathbf{k}} = v_F(|\mathbf{k}| - k_F)$, one can carry out the integration of eq. (8) with respect to \mathbf{k}' as follows:

$$\begin{aligned} \sum_{\mathbf{k}} \frac{1}{\xi_{\mathbf{k}}^2 + |\varepsilon_n|^2} &= \frac{1}{(2\pi)^2} \int d\mathbf{k} \frac{1}{v_F^2 (|\mathbf{k}| - k_F)^2 + |\varepsilon_n|^2} \\ &\simeq \frac{1}{2\pi} \int_{k_F - k_0}^{k_F + k_0} dk_F \frac{k}{v_F^2 (k - k_F)^2 + |\varepsilon_n|^2} \\ &= \frac{k_F}{\pi v_F |\varepsilon_n|} \tan^{-1} \frac{v_F k_0}{|\varepsilon_n|}. \end{aligned} \quad (9)$$

As mentioned above, the gap function must satisfy the following symmetry for the spin-singlet pairing

$$\Delta_d(\mathbf{k}, i\varepsilon_n) = \Delta_d(-\mathbf{k}, i\varepsilon_n) = \Delta_d(\mathbf{k}, -i\varepsilon_n) = \Delta_d(-\mathbf{k}, -i\varepsilon_n), \quad (10)$$

$$\Delta_p(\mathbf{k}, i\varepsilon_n) = -\Delta_p(-\mathbf{k}, i\varepsilon_n) = -\Delta_p(\mathbf{k}, -i\varepsilon_n) = \Delta_p(-\mathbf{k}, -i\varepsilon_n). \quad (11)$$

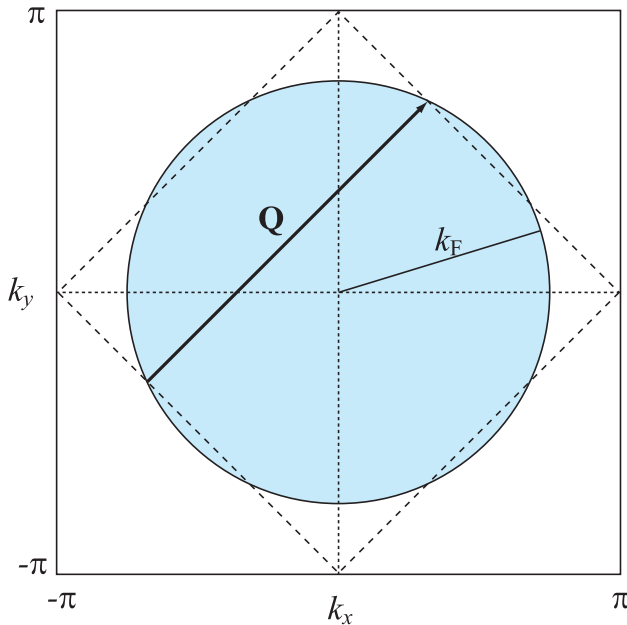


Fig. 2. Relation between the Fermi surface ($k_F = 0.75\pi$) and the ordering vector \mathbf{Q} .

Here we measure energies in unit of the Fermi energy ε_F . $g^2 N_F$ is set to be equal to ε_F throughout the paper. The Fermi surface (FS) is assumed to be two-dimensional circular with $k_F = 0.75\pi$ as is shown in Fig. 2. This simplified model may give clear understanding of a condition for the realization of the odd-frequency gap, although it does not corresponds to the practical Fermi surface of the heavy fermion compounds.

The transition temperature T_c is determined by condition $\lambda(T_c) = 1$. We have solved the eigenvalue problem (8) numerically by retaining 512 Matsubara frequency ε_n up to $|\varepsilon_n| \leq 131583\pi T$. The temperature dependences of the eigen value $\lambda(T)$'s are shown in Fig. 3. For the d -wave pairing, $\lambda(T)$ increases monotonously (logarithmically) as the temperature decreases as usual. For the p -wave odd-frequency pairing, on the other hand, $\lambda(T)$ exhibits a broad peak as shown in Fig. 3. Since this feature can be seen even in the case of the much larger cut-off frequency, it is not due to the cut-off frequency, but due to an intrinsic nature of the odd-pairing in frequency. Consequently, it is possible that there exist two temperatures T_c^\pm satisfying $\lambda(T_c^\pm) = 1$, so that the p -wave pairing is realized only in the temperature region $T_c^- < T < T_c^+$ (see the case $\eta = 0.05$ in Fig. 3). But in the case $\eta < 0.04$, λ does not fall below unity even for $T \rightarrow 0$, so that the p -wave pairing is realized in $0 \leq T < T_c^+$.

We recall that BA reached the analogous results for the odd-frequency pairing that the normal phase reappears below the lower- T_c . In the present model, we cannot show the existence of T_c^\pm , since the transition temperature for d -wave singlet pairing T_c^d is higher than T_c^+ for $\eta > 0.04$. The detailed analysis about the possibility of this multiple transition will be given in a subsequent

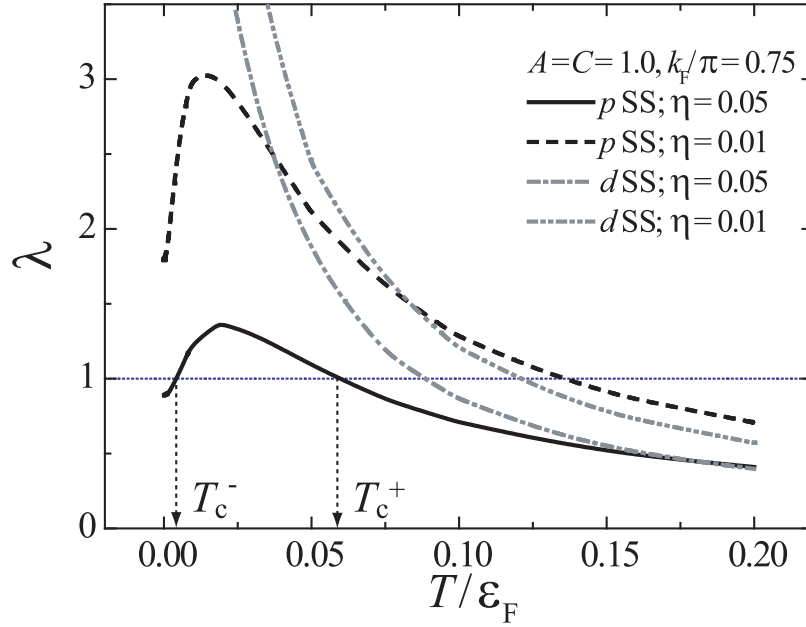


Fig. 3. Temperature dependence of the eigen value λ for p -wave singlet (p -S) and d -wave singlet (d -S).

paper.³³⁾

3. Competition between p -wave and d -wave pair states

As is shown in Fig. 4, the transition temperature for p -wave singlet T_c^p exceeds T_c^d when $\eta \lesssim 0.02$. That is to say, in the region away from the QCP, d -wave singlet pairing is realized and p -wave singlet pairing is formed very close to the QCP.

The reason why such p -wave singlet pairing arises near the AF-QCP can be understood as follows. The frequency dependence of $V_l(i\omega_m)$, which is calculated numerically by eq. (5), are shown in Fig. 5. As is also shown in Fig. 5, it should be reasonable to approximate the frequency dependence of $V_l(i\omega_m)$ as

$$V_l(i\omega_m) \simeq v_l \ln \frac{\omega_0}{\tilde{\eta} + |\omega_m|}. \quad (12)$$

Considering the symmetry property of the gap function, eqs. (10) and (11), we can express each V_l in the form:

$$V_p(i\varepsilon_n - i\varepsilon'_n) = \frac{v_p}{2} \left(\ln \frac{1}{\tilde{\eta} + |\varepsilon_n - \varepsilon'_n|} - \ln \frac{1}{\tilde{\eta} + |\varepsilon_n + \varepsilon'_n|} \right), \quad (13)$$

$$V_d(i\varepsilon_n - i\varepsilon'_n) = \frac{v_d}{2} \left(\ln \frac{1}{\tilde{\eta} + |\varepsilon_n - \varepsilon'_n|} + \ln \frac{1}{\tilde{\eta} + |\varepsilon_n + \varepsilon'_n|} \right). \quad (14)$$

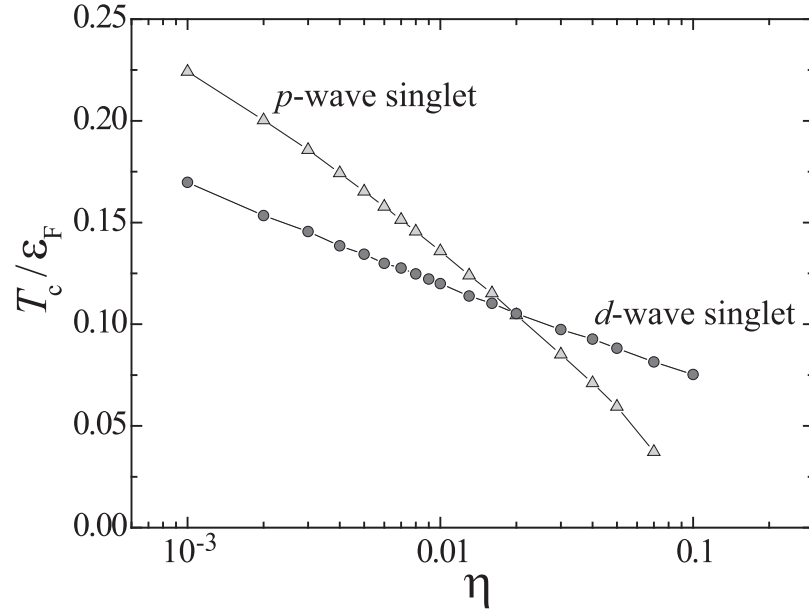


Fig. 4. Transition temperature for $p(d)$ -wave singlet pairing, $T_c^{p(d)}$, as a function of η .

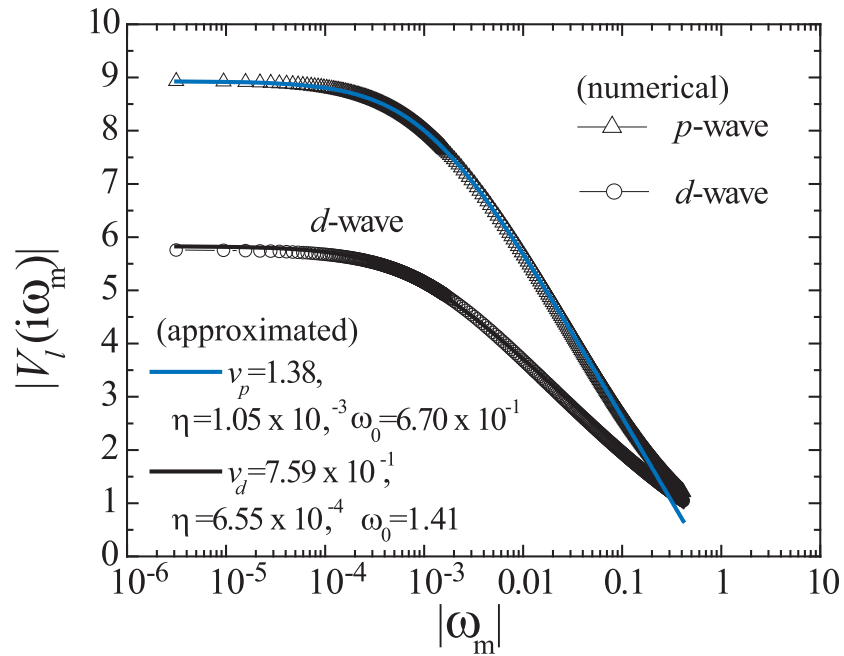


Fig. 5. Frequency dependence of $V_l(\omega_m)$

Let us consider the most singular case, $\varepsilon_n = \varepsilon'_n = \pi T$. Of course this example does not reproduce the present situation exactly, but gives a simple picture of the competition of the pairing states. Each V_l is given by

$$V_p(0) = \frac{v_p}{2} \ln \frac{\tilde{\eta} + 2\pi T}{\tilde{\eta}}, \quad (15)$$

$$V_d(0) = \frac{v_d}{2} \ln \frac{1}{\tilde{\eta}(\tilde{\eta} + 2\pi T)}. \quad (16)$$

When the system locates away from the QCP, i.e., $\tilde{\eta} \gg 2\pi T$,

$$V_p(0) \simeq \frac{v_p}{2} \frac{2\pi T}{\tilde{\eta}}, \quad (17)$$

$$V_d(0) \simeq \frac{v_d}{2} \left(-2 \ln \tilde{\eta} - \frac{2\pi T}{\tilde{\eta}} \right). \quad (18)$$

In this case, V_p is almost negligible compared to V_d , leading to $T_c^d \gg T_c^p$.

In contrast, when the system locates very close to the QCP, i.e., $\tilde{\eta} \ll 2\pi T$,

$$V_p(0) \simeq \frac{v_p}{2} \left(\frac{\tilde{\eta}}{2\pi T} - \ln \frac{\tilde{\eta}}{2\pi T} \right) \sim -\frac{v_p}{2} \ln \frac{\tilde{\eta}}{2\pi T}, \quad (19)$$

$$V_d(0) \simeq \frac{v_d}{2} \left(-2 \ln(2\pi T) - \frac{\tilde{\eta}}{2\pi T} - \ln \frac{\tilde{\eta}}{2\pi T} \right) \sim -\frac{v_d}{2} \ln \frac{\tilde{\eta}}{2\pi T}. \quad (20)$$

This time V_p is comparable to V_d , and in the case of $|v_p| > |v_d|$, T_c^p becomes higher than T_c^d .

As shown in Fig. 6, $|v_l|$ considerably depends on k_F . In other words, it is determined by the relation between the Fermi surface and AF ordering vector \mathbf{Q} . In the present case, the most singular pair scattering with $\mathbf{q} = \mathbf{Q} = (\pm\pi, \pm\pi)$ uses the points near $(\pm k_F/\sqrt{2}, \pm k_F/\sqrt{2})$, where the nodes of the d -wave pairing exists while that of the p -wave pairing does not. (See Fig. 7 (a), (b)) Therefore the effects of the singular pair scattering are suppressed in the case of d -wave pairing. This causes the relation $|v_p| > |v_d|$ in the present case.

Considering the above discussion, we can extend the condition of the emergence of the p -wave singlet pairing to the general case as following. Firstly, the pair scattering interaction must have a sharp peak in frequency whose width is smaller than the temperature (in the present case, $\eta \ll T$). Secondly, the most singular pair scattering with vector \mathbf{Q} has to be canceled out by the nodes of the d -wave pairing. In the case of Hubbard model at the half-filling, for example, the Fermi surface is nested with $\mathbf{Q} = (\pm\pi, \pm\pi)$ and the suppression of pair scattering becomes small, namely, $|v_p| \sim |v_d|$ (see Fig 7 (c)). So, it would be difficult for the p -wave singlet pairing to prevail over the d -wave singlet pairing on the Hubbard model, even near the AF-QCP. How about the cases of CeCu₂Si₂ and CeRhIn₅? The $1/T_1$ of both compounds rapidly increase approaching the AF+SC phase from SC phase.^{7,17} This indicates that the system is located very near the QCP, which would satisfy the first condition mentioned above. In CeRhIn₅, the most singular pair scattering vector is

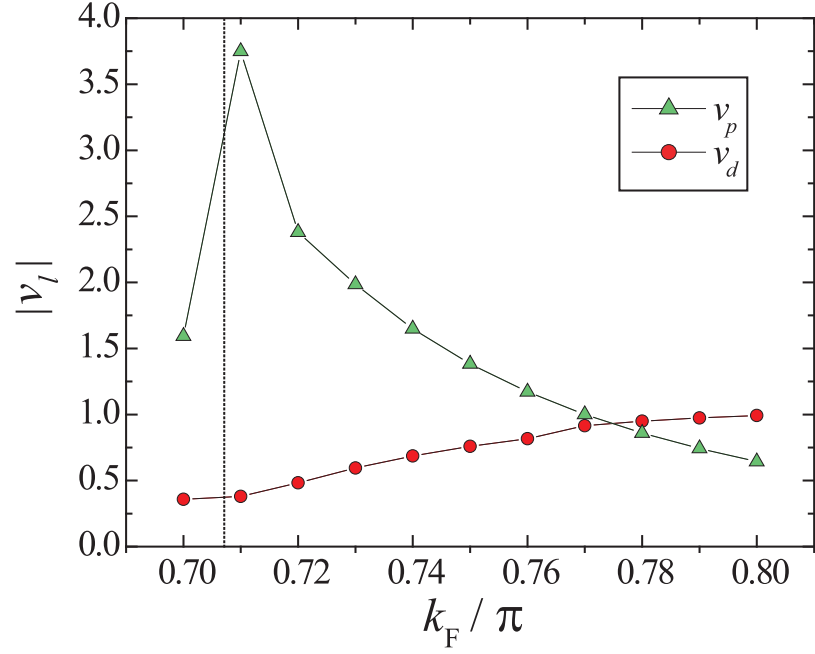


Fig. 6. k_F -dependence of v_l . The vertical dotted-line indicates $k_F = \pi/\sqrt{2}$ where $|\mathbf{Q}|$ is equivalent to the diameter of the Fermi surface.

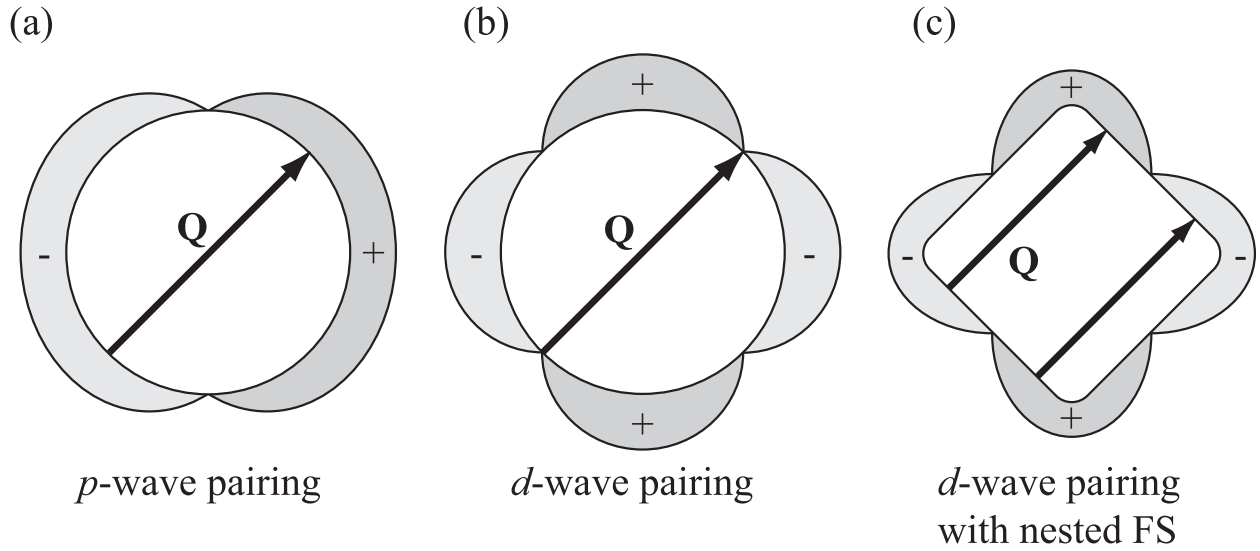


Fig. 7. Illustration of the relation between the AF ordering vector \mathbf{Q} and the position of the nodes. (a) *p*-wave pairing case: the most singular pair scattering with $\text{textbf}Q$ is not suppressed by the existence of the nodes. (b) *d*-wave pairing case: the scattering with \mathbf{Q} is suppressed by the existence of the nodes. (c) *d*-wave pairing with FS nested with \mathbf{Q} case: the suppression of pair scattering becomes small.

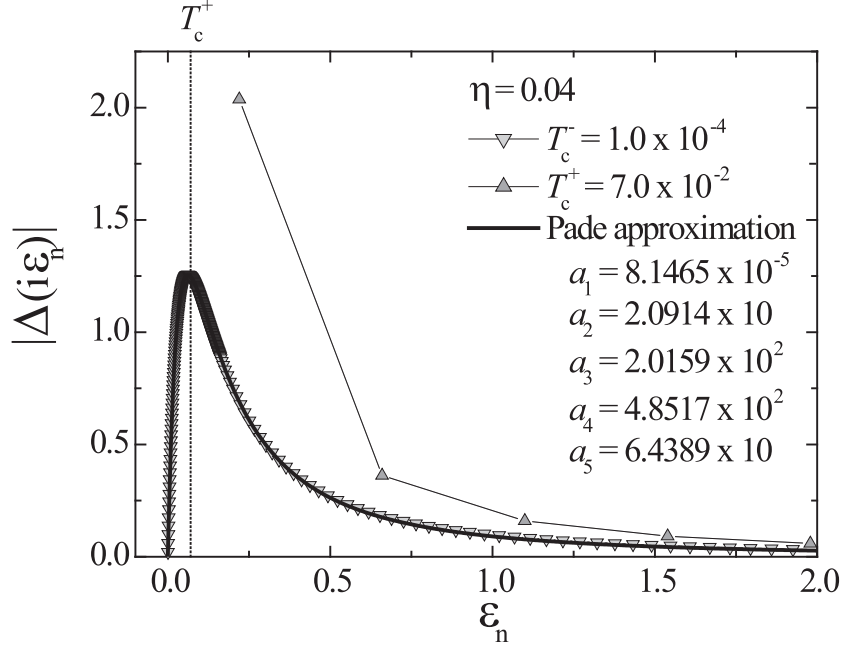


Fig. 8. Frequency dependence of the gap function of the p -wave singlet pairing at $T_c^+/\varepsilon_F = 7.0 \times 10^{-2}$ and $T_c^-/\varepsilon_F = 1.0 \times 10^{-4}$ for $\eta = 0.04$. The solid line indicates the results of Padé approximation.

$\mathbf{Q} = (\pi, \pi, 0.297\pi)$.³²⁾ Its Fermi surface does not nest in the direction \mathbf{Q} and is satisfied the relation $\mathbf{k}_F - \mathbf{k}'_F = \mathbf{Q}$ in the direction $(\pm 1, \pm 1, 0)$.³⁴⁾ The feature that \mathbf{Q} is independent from the nesting vector can be understood from the dual nature of electron. According to the itinerant-localized duality model,²¹⁾ the spin susceptibility $\chi(q, i\omega_m)$ is expressed in terms of the polarization function $\Pi(q, i\omega_m)$ of quasiparticles and the exchange interaction $J(q, i\omega_m)$ between localized component of electrons as follows:

$$\chi(q, i\omega_m)^{-1} = \chi_0(i\omega_m)^{-1} - 2\lambda^2 \Pi(q, i\omega_m) - J(q, i\omega_m), \quad (21)$$

where χ_0 is the local susceptibility expressing an effect of Kondo-like correlation, and λ is the renormalized spin-fermion coupling. Even if the Fermi surface is not nested, i.e., Π is not enhanced, the AF ordering can be triggered by $J(\mathbf{Q})$. Therefore, CeRhIn₅ would satisfy both conditions. In the case of CeCu₂Si₂, a situation is much more complicated ($\mathbf{Q} \sim (0.27\pi, 0.27\pi, 0.52\pi)$ ³⁵⁾), but its Fermi surface seems to satisfy the condition.³⁶⁾

4. Gaplessness of odd-frequency pairing

The frequency dependence of the gap function of the p -wave singlet pairing at $T_c^+ = 7.0 \times 10^{-2}$ and $T_c^- = 1.0 \times 10^{-4}$ for $\eta = 0.04$ are shown in Fig. 8. For $T = T_c^+$, at first sight, the gap seems to be divergent when ε_n approaches zero. The gap at $T = T_c^-$, on the other hand, has a peak at $\varepsilon_n^* = 6.19 \times 10^{-2}$, which is comparable to T_c^+ , and vanishes for $\varepsilon \rightarrow 0$, i.e., it exhibits a gapless-like

structure. This feature seems robust against variations of η , k_F or g . Therefore, we can suspect that the peak and the gapless-like structure is only hidden for $T = T_c^+$.

At the present stage, however, we cannot declare whether the present p -wave singlet gap function is completely gapless or not. So, we have to perform the analytic continuation of the gap function. In order to do that, first we apply the Padé approximation to the calculated gap function. Since the gap function is expected to be proportional to $|\varepsilon_n|^{-2}$ for large ε_n , we take the form:

$$\Delta_P(i\varepsilon_n) = \frac{a_5(\varepsilon_n + a_1)}{1 + a_2\varepsilon_n + a_3\varepsilon_n^2 + a_4\varepsilon_n^3}, \quad (22)$$

for $\varepsilon_n > 0$. We apply the least squares method to the calculated gap function $\Delta(i\varepsilon_n)$ by $\Delta_P(i\varepsilon_n)$ and obtain $a_1 = -1.2455 \times 10^{-5}$, $a_2 = 2.2966 \times 10$, $a_3 = 1.6980 \times 10^2$, $a_4 = 7.7980 \times 10^2$, $a_5 = 6.6046 \times 10$. Using these values of $a_{1\sim 5}$, we display $\Delta_P(i\varepsilon_n)$ in Fig. 8, in which $\Delta_P(i\varepsilon_n)$ shows a good agreement with $\Delta(i\varepsilon_n)$. The analytic continuation of this form becomes

$$\text{Re}\Delta_P(\varepsilon) = \frac{a_1 a_5 (1 - a_3 \varepsilon^2) + a_5 \varepsilon^2 (a_2 - a_4 \varepsilon^2)}{(1 - a_3 \varepsilon^2)^2 + \varepsilon^2 (a_2 - a_4 \varepsilon^2)}, \quad (23)$$

$$\text{Im}\Delta_P(\varepsilon) = \frac{a_5 \varepsilon (a_3 \varepsilon^2 - 1) + a_1 a_5 \varepsilon (a_2 - a_4 \varepsilon^2)}{(1 - a_3 \varepsilon^2)^2 + \varepsilon^2 (a_2 - a_4 \varepsilon^2)}. \quad (24)$$

From eqs. (23) and (24), the gap function at $\varepsilon = 0$ is reduced to $\text{Re}\Delta_P(0) = -8.2260 \times 10^{-4}$, $\text{Im}\Delta_P(0) = 0$. Therefore, we can conclude the present p -wave singlet superconductivity is a technically gapless one. We can determine the maximum of the gap, $\Delta_0(T)$ below T_c , by assuming that the gap has the same frequency dependence as that of the eigenfunction at $T \ll T_c$, where the eigenvalue λ exceeds unity further. Namely, $\Delta(i\varepsilon_n; T) \equiv \Delta_0(T) \Delta_P(i\varepsilon_n; T \ll T_c)$. At $T=0$, we obtained $\Delta_0(0)/T_c = 0.42$ (by setting parameters as $a_1 = -1.5256 \times 10^{-5}$, $a_2 = 4.6835 \times 10$, $a_3 = 6.4780 \times 10^2$, $a_4 = 2.8209 \times 10^3$, $a_5 = 1.1492 \times 10^2$, which corresponds to $\eta = 0.01$ case), which is much smaller than the BCS relation $\Delta_0(0)/T_c = 1.765$.

We can also discuss the gapless nature in more general form as follows. The linearized gap equation for the odd-frequency gap can be written as

$$\begin{aligned} \Delta_p(i\varepsilon_n) &= -N_F \int_{-\infty}^{\infty} d\xi T \sum_{\varepsilon'_n} \frac{V(i\varepsilon_n - i\varepsilon'_n)}{|\varepsilon'_n|^2 + \xi^2} \frac{1}{2} [\Delta_p(i\varepsilon'_n) - \Delta_p(-i\varepsilon'_n)] \\ &= -N_F \text{P} \int_{-\infty}^{\infty} \frac{dx}{8} \coth \frac{x}{2T} \frac{1}{x + i\varepsilon_n} [V(-x - i\delta) - V(-x + i\delta)] \times [\Delta(i\varepsilon_n + x) - \Delta(-i\varepsilon_n - x)] \\ &\quad - N_F \text{P} \int_{-\infty}^{\infty} \frac{dx}{8} \tanh \frac{x}{2T} \frac{1}{x + i\delta} [V(i\varepsilon_n - x) - V(i\varepsilon_n + x)] \times [\Delta(x + i\delta) - \Delta(-x - i\delta)]. \end{aligned} \quad (25)$$

The analytic continuation, $i\varepsilon_n \rightarrow \varepsilon + i\delta$ in eq. (26), results in the following gap equation:

$$\begin{aligned} \Delta(\varepsilon + i\delta) &= -N_F \text{P} \int_{-\infty}^{\infty} \frac{dx}{8} \left\{ \coth \frac{x - \varepsilon}{2T} [V(\varepsilon - x - i\delta) - V(\varepsilon - x + i\delta)] \right. \\ &\quad \left. + \tanh \frac{x}{2T} [V(\varepsilon - x + i\delta) - V(\varepsilon + x + i\delta)] \right\} \\ &\quad \times \frac{\Delta(x + i\delta) - \Delta(-x - i\delta)}{x + i\delta}. \end{aligned} \quad (27)$$

The analytic continuation of the effective pairing interaction $V_l(i\omega_m)$, (12), becomes

$$V(\omega + i\delta) = v_l \left(\ln \frac{\omega_0}{\sqrt{\omega^2 + \tilde{\eta}^2}} + i \tan^{-1} \frac{\omega}{\tilde{\eta}} \right) \quad (28)$$

Substituting eq. (28) into eq. (27), we obtain

$$\begin{aligned} \Delta(\varepsilon + i\delta) = & -v_l N_{FP} \int_{-\infty}^{\infty} \frac{dx}{8} \left\{ \tanh \frac{x}{2T} \ln \sqrt{\frac{(\varepsilon + x)^2 + \tilde{\eta}^2}{(\varepsilon - x)^2 + \tilde{\eta}^2}} \right. \\ & \left. + i \left[2 \coth \frac{x - \varepsilon}{2T} \tan^{-1} \frac{\varepsilon - x}{\tilde{\eta}} + \tanh \frac{x}{2T} \left(\tan^{-1} \frac{\varepsilon - x}{\tilde{\eta}} - \tan^{-1} \frac{\varepsilon + x}{\tilde{\eta}} \right) \right] \right\} \\ & \times \frac{\Delta(x + i\delta) - \Delta(-x - i\delta)}{x + i\delta}. \end{aligned} \quad (29)$$

Let us express the real (imaginary) part of the gap as $\Delta'(\varepsilon)$ ($\Delta''(\varepsilon)$), i.e., $\Delta(\varepsilon + i\delta) \equiv \Delta'(\varepsilon) + i\Delta''(\varepsilon)$. Then, each part of (29) are reduced to

$$\begin{aligned} \Delta'(\varepsilon) = & -v_l N_{FP} \int_{-\infty}^{\infty} \frac{dx}{8} \left\{ \tanh \frac{x}{2T} \ln \sqrt{\frac{(\varepsilon + x)^2 + \tilde{\eta}^2}{(\varepsilon - x)^2 + \tilde{\eta}^2}} \frac{\Delta'(x) - \Delta'(-x)}{x} \right. \\ & \left. - \left[2 \coth \frac{\varepsilon - x}{2T} \tan^{-1} \frac{\varepsilon - x}{\tilde{\eta}} + \tanh \frac{x}{2T} \left(\tan^{-1} \frac{\varepsilon - x}{\tilde{\eta}} - \tan^{-1} \frac{\varepsilon + x}{\tilde{\eta}} \right) \right] \frac{\Delta''(x) + \Delta''(-x)}{x} \right\} \end{aligned} \quad (30)$$

$$\begin{aligned} \Delta''(\varepsilon) = & -v_l N_{FP} \int_{-\infty}^{\infty} \frac{dx}{8} \left\{ \tanh \frac{x}{2T} \ln \sqrt{\frac{(\varepsilon + x)^2 + \tilde{\eta}^2}{(\varepsilon - x)^2 + \tilde{\eta}^2}} \frac{\Delta''(x) + \Delta''(-x)}{x} \right. \\ & \left. - \left[2 \coth \frac{\varepsilon - x}{2T} \tan^{-1} \frac{\varepsilon - x}{\tilde{\eta}} + \tanh \frac{x}{2T} \left(\tan^{-1} \frac{\varepsilon - x}{\tilde{\eta}} - \tan^{-1} \frac{\varepsilon + x}{\tilde{\eta}} \right) \right] \right. \\ & \left. \times \left[\frac{\Delta'(x) - \Delta'(-x)}{x} + \{ \Delta''(x) + \Delta''(-x) \} \pi \delta(x) \right] \right\}. \end{aligned} \quad (31)$$

Note here that we can show easily $\Delta'(\varepsilon) = -\Delta'(-\varepsilon)$, $\Delta(\varepsilon) = \Delta''(-\varepsilon)$. At $\varepsilon = 0$,

$$\Delta'(0) = 0, \quad (32)$$

$$\Delta''(0) = -v_l N_{FP} \int_{-\infty}^{\infty} \frac{dx}{2} \left(\coth \frac{x}{2T} - \tanh \frac{x}{2T} \right) \tan^{-1} \frac{x}{\tilde{\eta}} \cdot \frac{\Delta'(x)}{x} - v_l N_{FP} \pi \frac{T}{\tilde{\eta}} \Delta''(0). \quad (33)$$

From eq. (33),

$$\left(1 + v_l N_{FP} \pi \frac{T}{\tilde{\eta}} \right) \Delta''(0) = -v_l N_{FP} \int_{-\infty}^{\infty} \frac{dx}{2} \left(\coth \frac{x}{2T} - \tanh \frac{x}{2T} \right) \tan^{-1} \frac{x}{\tilde{\eta}} \cdot \frac{\Delta'(x)}{x}. \quad (34)$$

The right hand side of eq. (34) is constant, and $1 + v_l N_{FP} \pi T / \tilde{\eta} \rightarrow -\infty$ when $\tilde{\eta} \rightarrow 0$. Therefore, in order to satisfy eq. (34),

$$\Delta''(0) \rightarrow 0 \quad \text{for} \quad \tilde{\eta} \rightarrow 0 \quad (35)$$

is needed. From eqs. (32) and (35), we reach the fact that the present p -wave singlet gap function leads to an essentially gapless superconductivity at the QCP.

Considering the low-frequency structure of the gap function, we assume that the gap function can be approximate in the form:

$$\Delta(\mathbf{k}, i\omega_m) = \frac{\Delta_0}{T_c} i\omega_m \phi_p(\mathbf{k}). \quad (36)$$

Then we find from the poles of Green's function that

$$E_{\mathbf{k}} = \frac{\xi}{\sqrt{1 + (\Delta_0/T_c)^2 \phi_p^2(\mathbf{k})}}. \quad (37)$$

Therefore, the quasiparticle spectra with such gap function is gapless, i.e., there is no difference in excitations between the normal states and the present SC states, except for the effective mass enhancement:

$$m_{\mathbf{k}}^* = m \sqrt{1 + (\Delta_0/T_c)^2 \phi_p^2(\mathbf{k})}. \quad (38)$$

This mass enhancement is, however, very small due to the smallness of $\Delta_0/T_c \sim 0.42$ as mentioned above, so that the specific heat or the NMR relaxation rate does not show any significant change at T_c . This would correspond to the $1/T_1$ behavior observed in $\text{Ce}_{0.99}\text{Cu}_{2.02}\text{Si}_2$ ⁶⁻⁸) which shows almost the same behavior as the normal Fermi liquid state. If the $1/T_1 \propto T$ behavior is due to the impurity scattering, $1/T_1$ should shows a significant reduction at T_c and exhibit $1/T_1 \propto T$ well below T_c .³⁸) This is the reason why we conclude the $1/T_1 \propto T$ is not due to the impurity scattering but due to the odd-frequency gap.

5. Coexistence of AF and SC order

In the previous sections, we discussed the emergence of the gapless p -wave singlet pairing prevailing the d -wave singlet pairing in the paramagnetic (PM) backgrounds. The experimental results^{6-9, 16-19}) suggest that the gapless superconductivity is realized in the AF backgrounds rather than in the PM backgrounds. (In the SC phase very close to the phase boundary, the present theory predicts that the gapless p -wave singlet superconductivity is realized, but the detailed experimental results in this region have not been obtained yet.) Here we discuss that the gapless p -wave singlet can also be realized in rather wide region in AF+SC phase. Since the transverse spin susceptibility χ_{\perp} would be much dominant than the longitudinal one χ_{\parallel} , even if the damping effect would have been taken into account, the pairing interaction in the AF backgrounds may given as follows:

$$V(\mathbf{q}, i\omega_m) = g^2 \chi_{\perp}(\mathbf{q}, i\omega_m) \equiv \frac{g^2 N_F}{S^2 \hat{\mathbf{q}}^2 + |\omega_m|^2}, \quad (39)$$

where S corresponds to the spin-wave velocity. This interaction is similar to that just at QCP. Namely, the frequency dependence of $V_l^{\text{AF}}(i\omega_m)$ can be approximated as

$$V_l^{\text{AF}}(i\omega_m) \simeq v_l \ln \frac{\omega_0'}{|\omega_m|^2}. \quad (40)$$

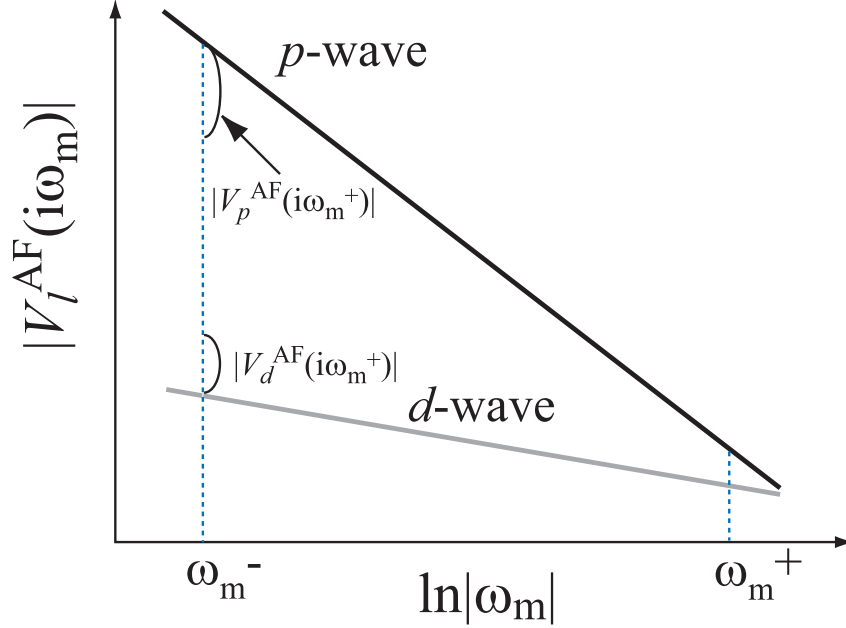


Fig. 9. Illustration of the frequency dependence of $V_l(i\omega_m)$ in the AF backgrounds, where $\omega_m^\pm \equiv \varepsilon_n \pm \varepsilon'_n$. The p -wave channel dominates the d -wave channel because $v_p > v_d$ and the unsaturated behavior of $V_l(i\omega_m)$.

Comparing this with the expression (12), the interaction V_l^{AF} of the AF side can be obtained by the transformation $V_l^{\text{AF}}(i\omega_m) \rightarrow 2V_l^{\text{PM}}(i\omega_m; \tilde{\eta} = 0)$. Figure 9 illustrates this situation. There is no saturation in contrast to V_l^{PM} in the PM side (see Fig. 5), which stimulates the emergence of p -wave singlet pairing. How the p -wave states dominate the d -wave one can be understood in the similar scenario discussed in §3, but this time we present much more generalized and intuitive picture about how the p -wave dominates the d -wave. Each V_l^{AF} can be expressed in the form

$$V_p^{\text{AF}}(i\omega_m) \simeq v_p \left(\ln \frac{1}{\omega_m^-} - \ln \frac{1}{\omega_m^+} \right) \quad (41)$$

$$V_d^{\text{AF}}(i\omega_m) \simeq v_d \left(\ln \frac{1}{\omega_m^-} + \ln \frac{1}{\omega_m^+} \right), \quad (42)$$

where $\omega_m^\pm \equiv \varepsilon_n \pm \varepsilon'_n$. From these expressions, we can easily find that $V_d^{\text{AF}} > V_p^{\text{AF}}$, in general, for $v_d \sim v_p$ because the first term and the second term are added for d -wave, while they offset each other for p -wave. In the case v_p is moderately larger than v_d as displayed in Fig. 9, however, the first term of V_p^{AF} is much larger than V_d^{AF} , so that the p -wave singlet pairing dominates the d -wave one. This situation would be realized easier in the AF side rather than that in the PM side because of the factor 2 and the unsaturation behavior of V_l^{AF} . Judging from above, no matter how the detail is, the p -wave pairing prevails d -wave one when the frequency dependence of the pairing interaction takes the form as shown in Fig. 9.

Below T_N , however, the energy gap is formed around the hot spot (Fig. 10) and the missing part of the Fermi surface spreads out as the AF ordering is developed. It leads to the remarkable

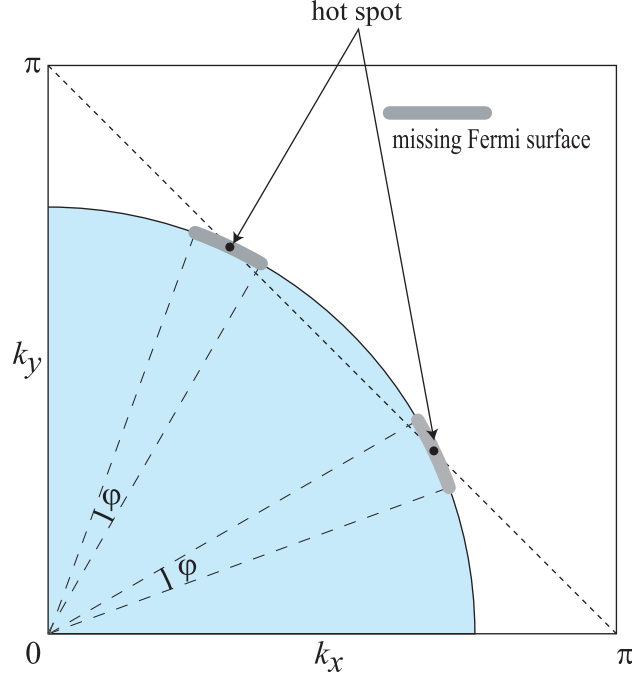


Fig. 10. Missing Fermi surface due to the AF energy gap and the definition of φ .

reduction of T_c because the dominant pair scattering is suppressed due to the existence of the AF gap. To simulate this situation, we parameterize the effect of the AF order as the angle φ of the missing part of the Fermi surface as displayed in Fig. 10. The growth of the AF gap, spreading of φ , deprives the pairing interaction of the most singular scattering with the AF ordering vector \mathbf{Q} , and suppresses V_l^{AF} . It is noted that this suppression is not the saturation effect displayed in Fig. 5, but the reduction of v_l . This reduction of v_l is remarkable for v_p , because the enhancement of v_p is mainly due to the scattering using the hot spots.

We can also discuss the gapless nature as discussed in §4. In the AF backgrounds, the pairing interaction V_l^{AF} is given by the same form as that in the PM backgrounds with $v_l \rightarrow 2v_l$ in the limit $\eta \rightarrow 0$. Thus we reach the same conclusion that the gap function in the AF side is always gapless:

$$\Delta'_{\text{AF}}(0) = 0, \quad (43)$$

$$\Delta''_{\text{AF}}(0) = 0. \quad (44)$$

Together with the T_c 's in the PM phase, the calculated T_c 's near the QCP are shown in Fig. 12 Here we set $S = 1.2$ and the other parameter $g^2 N_F$ and k_F to be the same as those in the PM backgrounds. In the PM region, the distance from the QCP is parameterized by η , and in the AF region, that is parameterized by φ . Indeed, the gap in AF backgrounds, shown in Fig. 11, has a gapless-like structure, and the parameters of Padé approximation are obtained as $a_1 = -3.3415 \times 10^{-3}$, $a_2 = 2.5624 \times 10$, $a_3 = -7.7475 \times 10$, $a_4 = 3.3734 \times 10^2$, $a_5 = 4.8612 \times 10$.

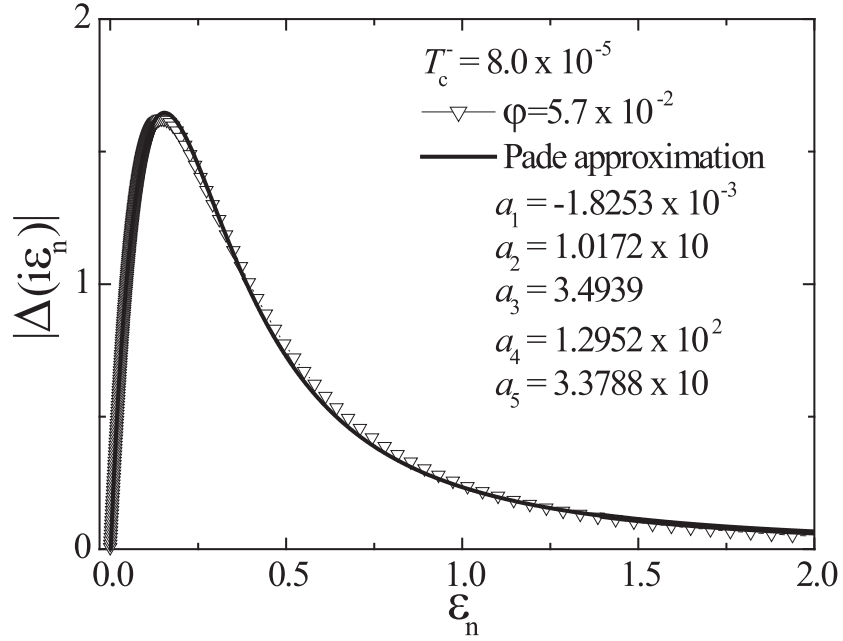


Fig. 11. Frequency dependence of the gap function of the p -wave singlet pairing in the AF background. The solid line indicates the results of Padé approximation.

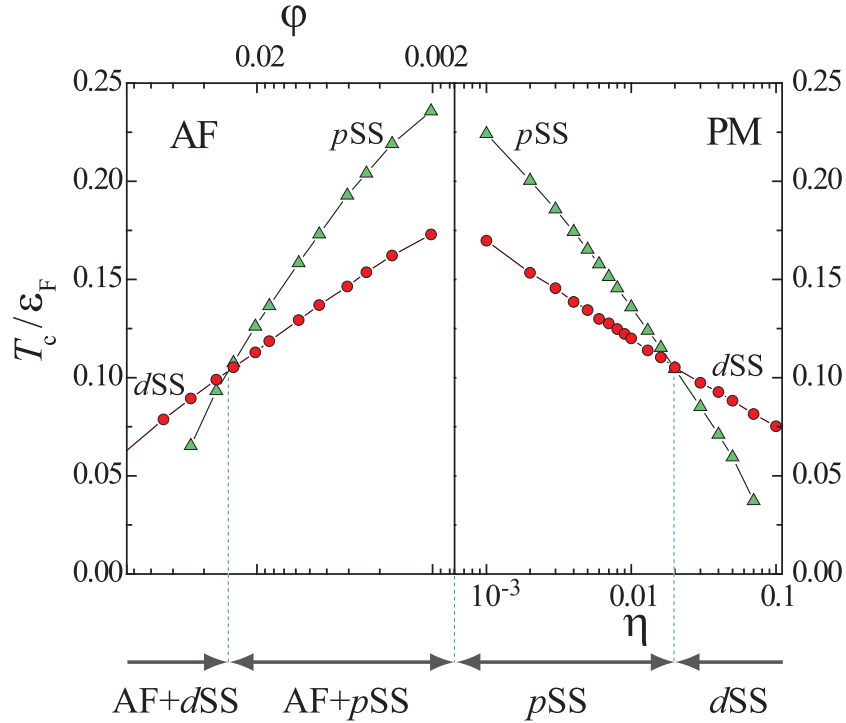


Fig. 12. Transition temperatures near the QCP. AF+dSC: d -wave singlet pairing (d -S) with line nodes; AF+pSC: gapless p -wave singlet (p -S); pSC: gapless p -S; dSC: d -S with line nodes.

The gapless odd-frequency p -wave singlet pairing is realized only near the QCP, and d -wave singlet pairing prevails p -wave singlet pairing in the PM region away from the QCP. According to this phase diagram, the observed $1/T_1$ may be explained as follows. Near the QCP, i.e., AF+ p SC and p SC region displayed in Fig. 12, $1/T_1$ does not show any significant reduction due to the gapless SC state. Away from the QCP (AF+ d SC and d SC region), $1/T_1 \propto T^3$ behavior is observed. This phase diagram agrees qualitatively with several experiments in CeCu₂Si₂ and CeRhIn₅. Polycrystalline sample of Ce_{0.99}Cu_{2.02}Si₂ shows gapless behavior at ambient pressure, and $1/T_1 \propto T^3$ behavior at pressures $P \gtrsim 0.1$ GPa.^{6,7)} This property can be understood that Ce_{0.99}Cu_{2.02}Si₂ at $P = 0$ GPa is located in p SC phase and at $P \gtrsim 0.1$ GPa, d SC phase. CeCu₂(Si_{0.99}Ge_{0.01})₂ compounds shows the AF ordering at $T < 0.75$ K, and below 0.5 K, the gapless superconductivity, coexisting with the AF order, at ambient pressure. This compounds also exhibits the line-node gap under the pressure $P = 0.85$ GPa.⁹⁾ Therefore, this compounds would be located in AF+ p SC phase at ambient pressure and in d SC phase at $P = 0.85$ GPa. The existence of p SC phase in this sample cannot be recognized from the present experimental data. Similarly, in CeRhIn₅ the pressure region $1.6 \lesssim P \lesssim 1.75$ GPa would correspond to AF+ p SC and $P > 2.1$ GPa would correspond to d SC.^{16–18)} For each case, the AF+ d SC phase, where the d -wave singlet SC states and the AF states coexist, have not been observed yet.

6. Conclusion

In the present paper, we have shown that the p -wave singlet superconductivity with the gap function which is odd in both momentum and frequency prevails the d -wave singlet superconductivity, at the AF-QCP and in the AF side of AF-QCP. This odd-frequency p -wave singlet pairing is stabilized in the AF states, and is able to coexist with the AF order. The characteristic properties of this p -wave singlet superconductivity is that i) there is no gap in the quasiparticle spectrum; ii) d -wave pairing arises apart from the AF-QCP even in the AF state; iii) In some parameter region, p -wave pairing is realized only in the window of temperatures $T_c^- < T < T_c^+$. The first and the second property would explain the experiments. Namely, the $1/T_1 \propto T$ behavior is observed in the AF+SC region or in the boundary of CeCu₂Si₂ or CeRhIn₅, and $1/T_1 \propto T^3$ behavior in the PM side away from the boundary. From the second one, we can predict that the d -wave pairing will be observed again away from the AF-QCP in the AF states.

The condition of the emergence of the p -wave singlet pairing is that the FS is not nested, so that the hot points of surface connected by the AF wave vector $\mathbf{Q} = (\pi, \pi)$ are isolated, while the AF order is induced by the exchange interaction between localized component of spin degrees of freedom. Although the structure of the Fermi surface of CeCu₂Si₂³⁶⁾ and CeRhIn₅³⁴⁾ is much more complicated than the present model, they seem to satisfy the condition from inspection of the shape of the Fermi surface obtained by band structure calculations. We thus believe that the

present theory would distill the fundamental picture of both CeCu_2Si_2 and CeRhIn_5 , and obtain the qualitative understanding of them. In order to get further understanding, extensive calculation considering the momentum-dependence and the practical dispersion of the quasiparticle are now in progress.

Acknowledgements

Authors would like to thank S. Kawasaki, G.-q. Zheng and Y. Kitaoka for discussion of experimental results. One of the authors (Y. F) is supported by Research Fellowships of the Japan Society for the Promotion of Science for Young Scientists. This work was supported by a Grant-in-Aid for COE Research (10CE2004) from Monbu-Kagaku-sho.

- 1) F. Steglich, J. Aarts, C. D. Bredl, W. Lieke, D. Meschede, W. Franz and H. Schäfer: Phys. Rev. Lett. **43** (1979) 1892.
- 2) K. Miyake, S. Schmitt-Rink and C. M. Varma: Phys. Rev. B **34** (1986) 6554.
- 3) D. J. Scalapino, E. Loh, Jr. and J. E. Hirsch: Phys. Rev. B **34** (1986) 8190.
- 4) K. Ueda, T. Moriya, Y. Takahashi: in *Electronic Properties and mechanism of High-Tc Superconductors* (Tsukuba Symposium, 1991) ed. T. Oguchi et al. (North Holland, 1992) p.145.
- 5) P. Monthoux and G. G. Lonzarich: Phys. Rev. B **59** (1999) 14598.
- 6) K. Ishida, Y. Kawasaki, K. Tabuchi, K. Kashima, Y. Kitaoka, K. Asayama, C. Geibel and F. Steglich: Phys. Rev. Lett. **82** (1999) 5353.
- 7) Y. Kawasaki, K. Ishida, T. Mito, C. Thessieu, G.-q. Zheng, Y. Kitaoka, C. Geibel and F. Steglich: Phys. Rev. B **63** (2001) 140501(R)
- 8) Y. Kitaoka, K. Ishida, Y. Kawasaki, O. Trovaelli, C. Geibel and F. Steglich: J. Phys.: Condens. Matter **13** (2001) L79.
- 9) Y. Kawasaki, K. Ishida, K. Obinata, K. Tabuchi, K. Kashima and Y. Kitaoka: Phys. Rev. B **66** (2002) 224502.
- 10) A. Koda, W. Higemoto, R. Kadono, Y. Kawasaki, K. Ishida, Y. Kitaoka, C. Geibel and F. Steglich: J. Phys. Soc. Jpn. **71** (2002) 1427.
- 11) F. Thomas, C. Ayache, I. A. Fomine, J. Thomasson and C. Geibel: J. Phys.: Condens. Matter **8** (1996) L51.
- 12) A. T. Holmes, A. Demuer and D. Jaccard: Proceedings of SCES'02, Acta Phys. Pol. B, in press.
- 13) Y. Onishi and K. Miyake: J. Phys. Soc. Jpn. **69** (2000) 3955.
- 14) H. Q. Yuan, M. Deppe, G. Sparn, F. M. Grosche, C. Geibel and F. Steglich: Proceedings of SCES'02, Acta Phys. Pol. B, in press.
- 15) H. Hegger, C. Petrovic, E. G. Moshopoulou, M. F. Hundley, J. L. Sarrao, Z. Fisk and J. D. Thompson: Phys. Rev. Lett **84** (2000) 4986.
- 16) T. Mito, S. Kawasaki, G.-q. Zheng, Y. Kawasaki, K. Ishida, Y. Kitaoka, D. Aoki, Y. Haga and Y. Ōnuki: Phys. Rev. B **63** (2001) 220506(R); cond-mat/0211576.
- 17) S. Kawasaki, T. Mito, G.-q. Zheng, C. Thessieu, Y. Kawasaki, K. Ishida, Y. Kitaoka, T. Muramatsu, T. C. Kobayashi, D. Aoki, S. Araki, Y. Haga, R. Settai and Y. Ōnuki: Phys. Rev. B **65** (2001) 020504; to be prepared.
- 18) Y. Kitaoka, Y. Kawasaki, T. Mito, S. Kawasaki, G.-q. Zheng, K. Ishida, D. Aoki, Y. Haga, R. Settai, Y. Onuki, C. Geibel and F. Steglich: J. Phys. Chem. Solids **63** (2002) 1141.
- 19) R. A. Fisher, F. Bouquet, N. E. Phillips, M. F. Hundley, P. G. Pagliuso, J. L. Sarrao, Z. Fisk and J. D. Thompson: Phys. Rev. B **65** (2002) 224509.
- 20) N. K. Sato, N. Aso, K. Miyake, R. Shiina, P. Thalmeier, G. Varelogiannis, C. Geibel, F. Steglich, P. Flude and T. Komatsubara: Nature **410** (2001) 340.
- 21) Y. Kuramoto and K. Miyake: J. Phys. Soc. Jpn. **59** (1990) 2381; Prog. Theor. Phys. Suppl. **108** (1992) 199; K. Miyake and Y. Kuramoto: Physica B **171** (1991) 20.
- 22) H. Tou, Y. Kitaoka, K. Asayama, C. Geibel, C. Schank and F. Steglich: J. Phys. Soc. Jpn. **64** (1995) 725.
- 23) G. Kotliar, E. Abrahams, A. E. Ruckenstein, C. M. Varma, P. B. Littlewood and S. Schmitt-Rink: Erophys. Lett. **15** (1991) 655.
- 24) K. Miyake and H. Maebashi: J. Phys. Chem. Solids **62** (2001) 53.
- 25) K. Miyake and O. Narikiyo: J. Phys. Soc. Jpn. **71** (2002) 867.

- 26) A. Balatsky and E. Abrahams: Phys. Rev. B **45** (1992) 13125.
- 27) V. L. Berezinskii, JETP Lett. **20** (1974) 287.
- 28) K. Miyake, T. Matsuura and H. Jichu: Prog. Theor. Phys. **72** (1984) 652.
- 29) Y. Kitaoka, K. Ueda, T. Kohara and K. Asayama: Solid State Commun. **51** (1984) 461.
- 30) E. Abrahams, A. Balatsky, J. R. Schrieffer and P. B. Allen: Phys. Rev. B **47** (1993) 513.
- 31) K. Miyake.: unpublished.
- 32) W. Bao, P. G. Pagliuso, J. L. Sarrao, J. D. Thompson, Z. Fisk, J. W. Lynn and R. W. Erwin: Phys. Rev. B **62** (2000) R14621.
- 33) Y. Fuseya, H. Kohno and K. Miyake: in preparation.
- 34) R. Settai, H. Shishido, S. Ikeda, Y. Murakawa, M. Nakashima, D. Aoki, Y. Haga, H. Harima and Ōnuki: J. Phys.: Condens. Matter **13** (2001) L627.
- 35) G. Knebel, C. Eggert, D. Engelmann, R. Viana, A. Krimmel, M. Dressel and A. Loidl: Phys. Rev. B **53** (1996) 11586.
- 36) H. Harima and A. Yanase: J. Phys. Soc. Jpn. **60** (1991) 21.
- 37) The similar properties that the peak position of the gap is scaled by T_c is also seen in the odd-energy gap function in one-dimensional case as is seen in Y. Fuseya, H. Kohno and K. Miyake: J. Phys.: Condens. Matter **14** (2002) L655.
- 38) For example, K. Ishida, H. Mukuda, Y. Kitaoka, Z. Q. Mao, Y. Mori and Y. Maeno: Phys. Rev. Lett. **84** (2000) 5387.